Journal of Alloys and Compounds 512 (2012) 195–198

Contents lists available at SciVerse ScienceDirect

Journal of Alloys and Compounds

journal homepage: www.elsevier.com/locate/jallcom

Evidence of room temperature ferromagnetism in Co-doped transparent $CuAlO_2$ semiconductor

C.J. Dong [a,b,c], W.X. Yu [a], M. Xu [c], J.J. Cao [b,d], Y. Zhang [b], Y.H. Chuai [b], Y.D. Wang [b,*]

[a] Department of Materials Science, Jilin University, Changchun 130012, PR China
[b] State Key Laboratory on Integrated Optoelectronics, College of Electronic Science and Engineering, Jilin University, Changchun 130012, PR China
[c] Laboratory for Information Materials, College of Electrical & Information Engineering, Southwest University for Nationalities, Chengdu 610041, PR China
[d] College of Physics, Jilin University, Changchun 130012, PR China

ARTICLE INFO

Article history:
Received 8 August 2011
Received in revised form
19 September 2011
Accepted 20 September 2011
Available online 24 September 2011

Keywords:
$CuAlO_2$
Co-doped
Delafossite structure
Ferromagnetism

ABSTRACT

We synthesized $CuAl_{1-x}Co_xO_2$ (x = 0.00–0.07) thin films by solid-state reaction from Cu_2O and Al_2O_3 on a sapphire (0 0 1) substrate by a simple and cost-effective spin-on technique. X-ray diffraction and Raman spectroscopy confirm the formation of single impurity-free delafossite $CuAlO_2$ structure for all the compositions. We observed diamagnetism for pristine $CuAlO_2$ and ferromagnetism for Co-doped $CuAlO_2$ at room temperature. Specially, the coercivity (H_c) and saturation magnetization (M_s) are significantly enhanced with Co composition from 1 at.% to 5 at.% but show the reverse tendency with higher Co content.

1. Introduction

Much attention has been focused on diluted magnetic semiconductors (DMSs) with Curie temperature (TC) at or above room temperature (RT), since both the charge and spin of the carriers can be controlled in the same material simultaneously [1]. Particularly, oxide-based DMSs such as ZnO [2–4], SnO_2 [5,6], In_2O_3 [7,8], and TiO_2 [9,10] doped with different transition metals (TMs) have been widely studied following the theoretical prediction by Dietl et al. of RT ferromagnetism in Mn-doped ZnO and GaN [11]. Although there is a wholly new class of semiconductors, most experimental and theoretical efforts so far have mainly focused on *n*-type oxide semiconductors, ignoring the existence of p-type oxide-based DMSs. A recently discovered transparent p-type oxide semiconductor, $CuAlO_2$, with wide band gap energies of about 3.5 eV (direct) and 1.8 eV (indirect) [12], could open a range of novel applications. This finding suggests that the delafossite $CuAlO_2$ phase has the advantage of possessing two cation sites, Cu^{1+} and Al^{3+}, for possible magnetic ion substitution. Subsequently, magnetic properties of Mn-doped transparent $CuAlO_2$ semiconductors have been discussed [13]. In addition, theoretical first-principles calculations based on $CuAlO_2$ show that the ferromagnetic states of $(Cu,Co)AlO_2$ are highly stable, which makes them candidates for ferromagnetic DMSs [14]. Yet, there is still a lack of experimental data available on the Co-doped $CuAlO_2$ semiconductor, which motivates further studies. Theoretical and experimental exploring the magnetic behavior in Co-doped $CuAlO_2$ semiconductor will facilitate its potential applications such as spin-based light emitting diodes, spin-valve transistors, nonvolatile memory and detectors in spintronic devices.

In this work, we synthesize Co-doped $CuAlO_2$ by solid-state reaction from Cu_2O and Al_2O_3. We systematically study the influence of Co composition on the magnetic properties of $CuAl_{1-x}Co_xO_2$ with varying x prepared via the same method. The growth of $CuAlO_2$ films with highly (0 0 6)-preferred orientation that we have achieved will help to develop $CuAlO_2$ based DMS materials.

2. Experimental methods

2.1. Synthesis

We synthesized $CuAl_{1-x}Co_xO_2$ films with x = 0.00, 0.01, 0.03, 0.05, and 0.07 by solid-state reaction on a sapphire (0 0 1) substrate. A stoichiometric mixture of Cu_2O, Al_2O_3, and $Co(CH_3COO)_2{\cdot}4H_2O$ powders with 99.99% purity was milled for 10 h, and then was mixed with a proper amount of ethyl-cellulose (EC) and terpineol widely used in screen-printing. The films were spin-coated onto sapphire (0 0 1) substrates at a speed of 8000 rpm for 30 s. The samples were then dried at 60 °C for 10 min, and then preheated at 350 °C for 3 h to evaporate the solvent and remove organic residues in air. Finally, all deposited films were annealed at 1150 °C for 1 h in a corundum tube furnace, and a natural cooling was maintained after annealing was finished. Before deposition, sapphire substrates were cleaned sequentially with

* Corresponding author. Tel.: +86 431 85168240; fax: +86 431 85168240.
E-mail address: wangyiding47@yahoo.com.cn (Y.D. Wang).

0925-8388/$ – see front matter © 2011 Elsevier B.V. All rights reserved.
doi:10.1016/j.jallcom.2011.09.062

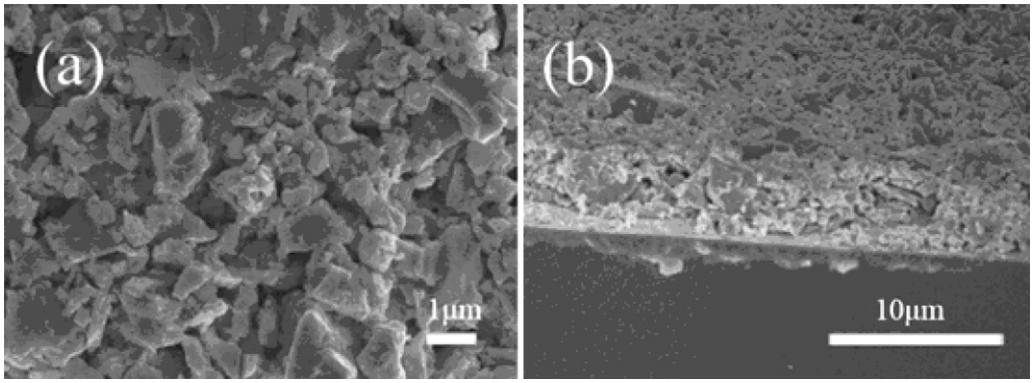

Fig. 1. FESEM surface micrograph and cross-sectional image of pristine $CuAlO_2$ film.

acetone, ethanol, and deionized water in an ultrasonic cleaner. Because of the low Co content, the weighing error was lessened by increasing the molar fraction of reagents. Furthermore, a physical balance with a precision of three decimal figures was used for weighing.

2.2. Characterization

We structurally characterized the obtained products via X-ray diffraction (XRD) using a Bruker D8 Advance with an incident X-ray wavelength of 1.540 Å. To study the surface and cross-section morphology of films, field emission scanning electron microscopy (FESEM) images were taken using a JEOL JEM-6700F microscope. A vibrating sample magnetometer (Lake Shore7410) was used for the room temperature magnetic measurements. We further studied the surface chemical composition and bonding states using X-ray photoelectron spectroscopy (XPS) with a monochromated Alα ($h\nu$ = 1486.7 eV) source. All the XPS spectra were calibrated using the C 1s peak (284.6 eV).

3. Results and discussion

3.1. Microstructure and crystal structure

Fig. 1 shows the FESEM images of the surface and cross-section morphology of pristine $CuAlO_2$ film. Note (Fig. 1(a)) that the $CuAlO_2$ grain size is not uniform on the order of microns but free from porosity. The film cross-section image (Fig. 1(b)) displays consecutive structures with an average height of ~5 μm standing on the substrate. Particularly, no obviously different patterns are observed in the case of Co-doped $CuAlO_2$ (not shown here). These results show the feasibility of growing $CuAlO_2$ film using spin-coating from mixed powder helped by proper EC and terpineol solvent.

The XRD patterns of the $CuAl_{1-x}Co_xO_2$ films, shown in Fig. 2, provide convincing evidence that the samples are all single-phase delafossite $CuAlO_2$ (space group: $R\bar{3}m$), which matches well with JCPDS card 77-2493 [15]. No diffraction peak corresponding to any other secondary phase, such as Co (JCPDS card 05-0727) or CoO (JCPDS card 48-1719) [16], CuO (JCPDS card 48-1548) [17], can be observed in any of the patterns, thereby showing the absence of detectable Co clusters and any other possible secondary phases. This means that the Co has been doped into the $CuAlO_2$ crystal structure to form a solid solution. Note that all the relative peak intensities of Co-doped samples are similar, especially for (0 0 6) peaks, which implies that no crystal structure change occur because of the similar radius size between Co^{2+} and Al^{3+} as discussed below. We found both lattice parameters a and c to increase slightly from 2.856 to 2.864 Å and 16.850 to 16.943 Å, respectively, as the concentration of Co is increased from 0 to 7 at.%. We used X-ray photoelectron spectroscopy (XPS) to determine that the Co was in the +2 oxidation state, since the radius of Co^{2+} (0.58 Å) [18] is always smaller than that of Cu^{1+} (0.95 Å) but slightly larger than that of Al^{3+} (0.55 Å) [13]. As such, the decrease of c could be detected if Co ions were substituted at the Cu sites. Thus, it is reasonable to conclude that Co ions substitute for the Al site but not the Cu site. Moreover, previous synthesis of $CuCoO_2$ [19,20] confirms our conclusion.

3.2. Raman spectra and XPS analysis

We further checked the quality of our $CuAl_{1-x}Co_xO_2$ films using Raman spectroscopy. Fig. 3(a) shows an RT first-order Raman spectrum of the pristine $CuAlO_2$ and $CuAl_{0.95}Co_{0.05}O_2$ obtained with 514.5-nm laser excitation. We clearly see the $A_{1g} + E_g$ symmetry configuration arising from the structure of $CuAlO_2$. In Fig. 3(a), we observe two intense peaks at 418.92 cm^{-1} (FWHM: 6.27 cm^{-1}) and 766.47 cm^{-1} (FWHM: 10.04 cm^{-1}) for pristine $CuAlO_2$, which we identify as the E_g and A_{1g} modes of $CuAlO_2$ by comparing with other results [21,22]. We also observe E_g and A_{1g} peaks at 417.36 cm^{-1} (FWHM: 6.71 cm^{-1}) and 766.42 cm^{-1} (FWHM: 9.36 cm^{-1}) for $CuAl_{0.95}Co_{0.05}O_2$ film. Again, these results confirm the existence of delafossite-phase $CuAlO_2$ films, because there are

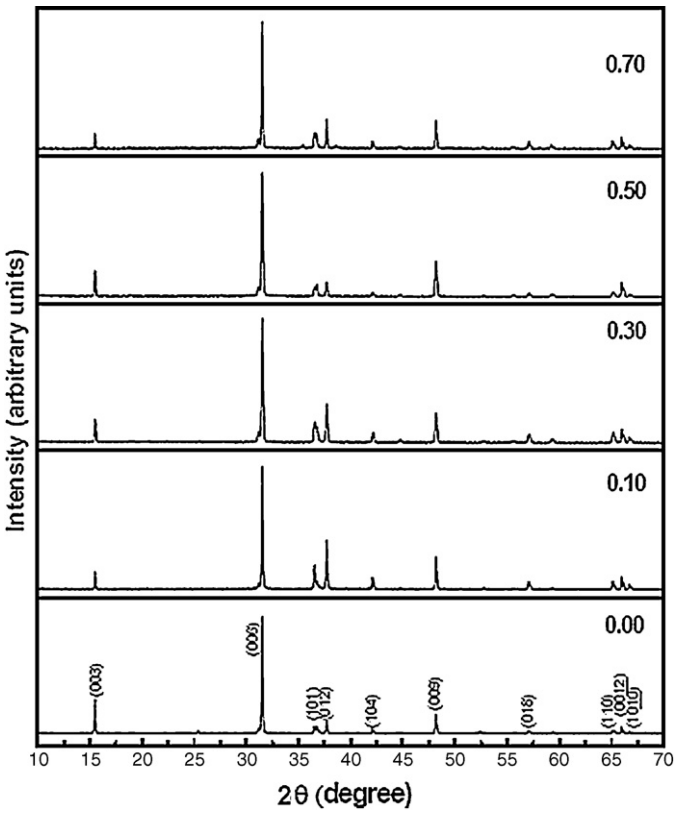

Fig. 2. XRD patterns of $CuAl_{1-x}Co_xO_2$ films (x = 0.00, 0.01, 0.03, 0.05, and 0.07).

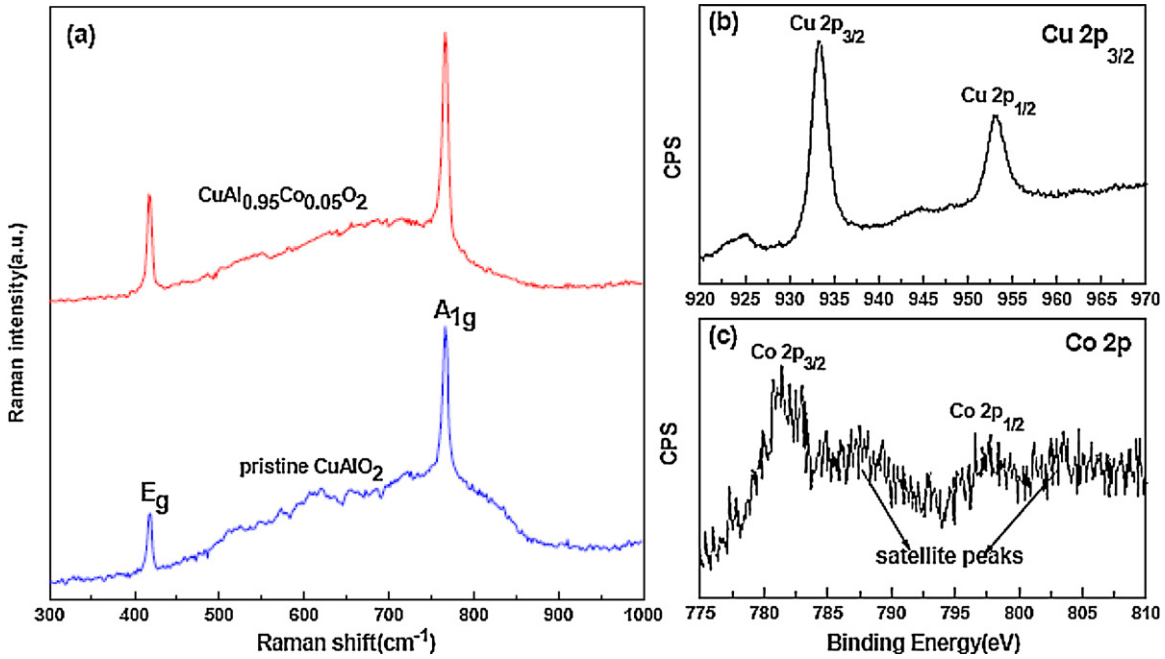

Fig. 3. Raman spectra of pure $CuAlO_2$ and $CuAl_{0.95}Co_{0.05}O_2$ films recorded under 514.5-nm excitation (a). Typical XPS scans of the Cu 2p (b) and Co 2p (c) spectral regions for $CuAl_{0.95}Co_{0.05}O_2$ film.

no Co-related or CuO peaks. This further supports our conclusion from XRD that the Co-doped $CuAlO_2$ films consist only of the single phase.

XPS verifies the presence of Co ions in these $CuAl_{1-x}Co_xO_2$ films, and Fig. 3(c) shows a typical spectrum for $CuAl_{0.95}Co_{0.05}O_2$. We accurately calibrated all XPS spectra with the C1 s peak at 284.6 eV from contamination to compensate the charge effect. For the $CuAl_{0.95}Co_{0.05}O_2$ sample, the core level of Co $2p_{3/2}$ was located at 780.8 eV, and that for Co $2p_{1/2}$ peak was at 796.2 eV. However, no trace of Co metallic precipitation (with $2p_{3/2}$ binding energy of 777.8 eV and $2p_{1/2}$ binding energy of 792.5 eV [23]) was observed in the spectra. This phenomenon is also seen in Co-doped ZnO [3] and SnO_2 [6]. Additionally, the satellite peaks due to the interaction between the core hole and the valence electron at 787.6 eV and 803.3 eV exclude the presence of Co^{3+}. Thus, this shows that the substituted Co is in the +2 oxidation state, comparable to that of Co^{2+} in CoO [24]. Moreover, the Cu 2p spectra are dominated by a simple spin-orbit slit doublet of Cu $2p_{3/2}$ and Cu $2p_{1/2}$, as also shown in Fig. 3(b). The Cu $2p_{3/2}$ component is found at 933.2 eV binding energy and has a FWHM of about 1.73 eV. This corresponds to a Cu $3d^{10}$ configuration in the final state deriving from Cu^{1+}, which agrees well with other studies [25,26]. The O 1s peak at 531.2 eV and Al 2p peak at 74.3 eV correspond to the valence states −2 for oxygen and +3 for aluminum (not shown here). We obtained similar results for the other $CuAl_{1-x}Co_xO_2$ samples. Note that no trace of the CuO phase was found through any of the above analyses. Hence, those samples were used for the following magnetic measurements.

3.3. Magnetic properties

Magnetization hysteresis loops of the $CuAl_{1-x}Co_xO_2$ films measured at RT are shown in Fig. 4. Both experiment and calculation indicate that the ferromagnetism of Cu-doped ZnO is caused principally by the strong p-d exchange interaction between O 2p and Cu 3d orbitals [2,4]. However, the magnetic measurements of the pristine $CuAlO_2$ sample show nearly straight lines (shown in the inset of Fig. 4(a)), indicating diamagnetism, which shows the impossibility of magnetism for intrinsic $CuAlO_2$. Conversely, the *M*–*H* loops

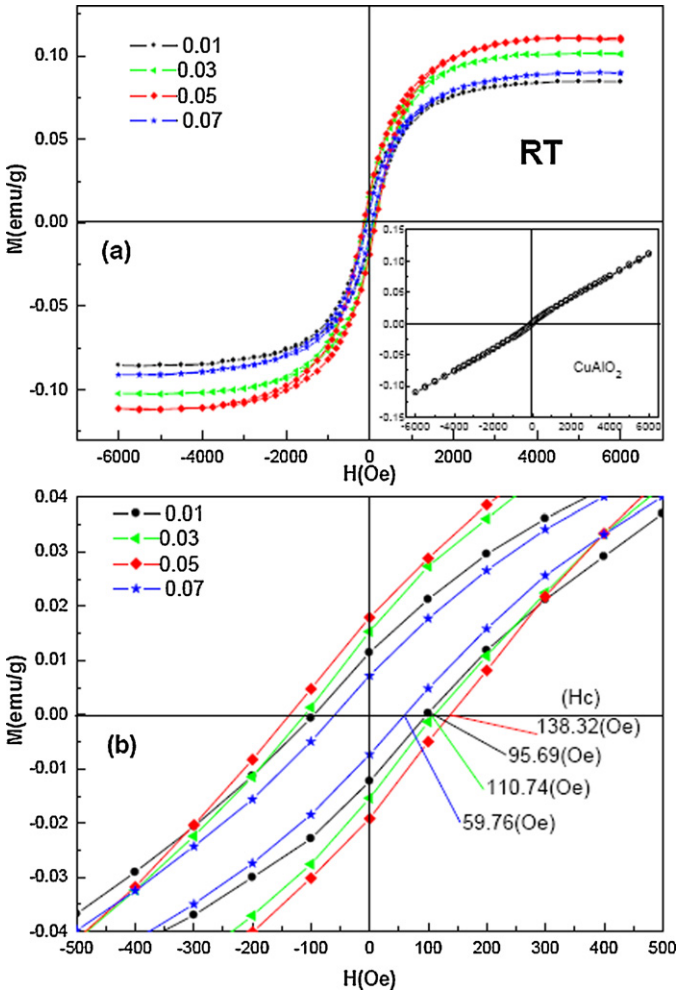

Fig. 4. (a) RT *M* vs *H* curves of studied samples (the inset shows the relevant curve for pristine $CuAlO_2$), and (b) enlarged view of the corresponding low-field region.

with Co-doped $CuAlO_2$ have a well-defined S-shape, convincingly showing ferromagnetic ordering at RT. We see that the coercivity (H_c) values are approximately 95.69, 110.74, and 138.32 Oe for Co composition of 0.01, 0.03, and 0.05, respectively, clearly showing RT ferromagnetism. Meanwhile, the saturation magnetizations (M_s) are around 0.084, 0.101, 0.110, and 0.089 emu/g, and the remnant magnetizations (M_r) are about 0.012, 0.015, 0.019, and 0.007 emu/g for the $CuAl_{1-x}Co_xO_2$ samples with Co compositions of 0.01, 0.03, 0.05, and 0.07, respectively, showing a slight attenuation with an increase in Co concentration. These data also yield insight into the changes in magnetic properties caused by the increase in Co concentration. In particular, one of the key features is that the $CuAl_{0.93}Co_{0.07}O_2$ samples show clear hysteresis with a decreased coercivity of about 59.76 Oe, and also show a drop of saturation magnetization and remnant magnetizations simultaneously. The highest M_s observed is 0.110 emu/g for 5 at.% Co-doped $CuAlO_2$ film, and the corresponding magnetic moment per Co atom was estimated to be about $0.02\mu_B$. This value is much lower than the expected value of $3\mu_B/Co^{2+}$ for tetrahedrally coordinated high-spin Co^{2+} ions.

The RT ferromagnetism in our case is not supposed to arise from the metallic Co phase clusters, nor from any secondary cobalt oxide phases ruled out by XRD, Raman and XPS measurements together. Moreover, Cobalt oxide (CoO) is well known to be paramagnetic above the Ne'el temperature of 291 K [27], and the observed ferromagnetic results from the CuO phase go up only to 330 K [28]. Consequently, RT ferromagnetic behavior of the sample might not be explained in terms of the formation of CoO or CuO. Thus, the observed ferromagnetism is essentially intrinsic to some extent. The origin of ferromagnetism in DMSs is still not very clear, although many efforts have been made to explain it. It is believed from the calculated density of states (DOS) that the double exchange interaction is the dominant exchange mechanism in TM-doped $CuAlO_2$-based DMSs [14]. It is also found that indirect interaction among Co centers results in ferromagnetism, whereas direct interaction among them induces antiferromagnetism [11,29]. Therefore, the increased antiferromagnetic superexchange interaction between Co moments at higher Co concentration could also be a cause for this decrease in saturation magnetization, because the average distance between Co ions decreases. Similar phenomena have also been seen in Co-doped ZnO [3]. Once synthesized, the manipulation of DMSs into a useful state needs appropriate doping concentration. On the other hand, a low-temperature paramagnetic moment has been reported that is consistent with a spin-1/2 defect with a density of 3.4×10^{20} cm^{-3}, probably due to Cu vacancies [30]. Recently, it is proposed that the polarised unpaired electrons nearby defects may be responsible for the weak magnetism of the material [31]. So, native defects, carrier concentration, and Co doping with other elements or TMs together significantly affect oxide-based DMSs. Therefore, P-type $CuAlO_2$-based DMSs remain an open question, and further experimental and theoretical studies are highly expected. Sophisticated understanding on magnetic properties in $CuAlO_2$ semiconductor is great promising for designing the $CuAlO_2$-based DMSs in spintronic devices.

4. Conclusions

In summary, we synthesized thin films of $CuAl_{1-x}Co_xO_2$ with $x = 0.00$, 0.01, 0.03, 0.05, and 0.07 on a sapphire substrate using a spin-on technique assisted by proper EC and terpineol solvent. FESEM measurements showed an average grain size on the order of microns and a thickness of about ~5 μm. XRD patterns and Raman spectra confirm single delafossite structure for all the films. XPS analysis suggests that Co is present in the +2 oxidation state in the Co-doped $CuAlO_2$ matrix and results in an intrinsic ferromagnetism in opposition to diamagnetism for pristine $CuAlO_2$ at RT. The variation of RT ferromagnetism with Co content shows the importance of appropriate substitution for $CuAlO_2$-based DMS application, but much more effort is needed to explore the magnetic properties of $CuAlO_2$-based DMSs.

References

[1] S.A. Wolf, D.D. Awschalom, R.A. Buhrman, J.M. Daughton, S.von. Molna'r, M.L. Roukes, A.Y. Chtchelkanova, D.M. Treger, Science 294 (2001) 1488.
[2] M. Ferhat, A. Zaoui, R. Ahuja, Appl. Phys. Lett. 94 (2009) 142502.
[3] Y.C. Qiu, W. Chen, S.H. Yang, B. Zhang, X.X. Zhang, Y.C. Zhong, K.S. Wong, Cryst. Growth Des. 10 (2010) 177.
[4] A. Tiwari, M. Snure, D. Kumar, J.T. Abiade, Appl. Phys. Lett. 92 (2008) 062509.
[5] C.B. Fitzgerald, M. Venkatesan, L.S. Dorneles, R. Gunning, P. Stamenov, J.M.D. Coey, P.A. Stampe, R.J. Kennedy, E.C. Moreira, U.S. Sias, Phys. Rev. B 74 (2006) 115307.
[6] W.B. Chen, J.B. Li, J. Appl. Phys. 109 (2011) 083930.
[7] X.Q. Meng, L.M. Tang, J.B. Li, J. Phys. Chem. C 114 (2010) 17569–17573.
[8] F.X. Jiang, X.H. Xu, J. Zhang, X.C. Fan, H.S. Wu, M. Alshammari, Q. Feng, H.J. Blythe, D.S. Score, K. Addison, M.A. Qahtani, G.A. Gehring, J. Appl. Phys. 109 (2011) 053907.
[9] Y. Matsumoto, M. Murakami, T. Shono, T. Hasegawa, T. Fukumura, M. Kawasaki, P. Ahmet, T. Chikyow, S. Koshihara, H. Koinuma, Science 291 (2001) 854.
[10] S. Sharma, S. Chaudhary, S.C. Kashyap, S.K. Sharma, J. Appl. Phys. 109 (2011) 083905.
[11] T. Dietl, H. Ohno, F. Matsukura, J. Cibert, D. Ferrand, Science 287 (2000) 1019.
[12] H. Kawazoe, M. Yasukawa, H. Hyodo, M. Kurita, H. Yanagi, H. Hosono, Nature 389 (1997) 939.
[13] H.Y. Zhang, P.G. Li, C.P. Chen, Q.Y. Tu, W.H. Tang, J. Alloys Compd. 396 (2005) 40–43.
[14] H. Kizaki, K. Sato, A. Yanase, H. Katayama-Yoshida, Jpn. J. Appl. Phys. 44 (2005) L1187–L1189.
[15] T. Prakash, K. Padma Prasad, R. Kavitha, S. Ramasamy, B.S. Murty, J. Appl. Phys. 102 (2007) 104104.
[16] K. An, N. Lee, J. Park, S.C. Kim, Y. Hwang, J.G. Park, J.Y. Kim, J.H. Park, M.J. Han, J. Yu, T. Hyeon, J. Am. Chem. Soc. 128 (2006) 9753–9760.
[17] C. Díaz-Guerra, M. Vila, J. Piqueras, Appl. Phys. Lett. 96 (2010) 193105.
[18] O.D. Jayakumar, C. Sudakar, C. Persson, H.G. Salunke, R. Naik, A.K. Tyagi, Appl. Phys. Lett. 97 (2010) 232510.
[19] R.D. Shannon, D.B. Rogers, C.T. Prewitt, Inorg. Chem. 10 (1971) 713.
[20] M. Beekmana, J. Salvadorb, X. Shic, G.S. Nolasa, J. Yangb, J. Alloys Compd. 489 (2010) 336–338.
[21] J. Pellicer-Porres, D. Martínez-García, A. Segura, P. Rodríguez-Hernández, A. Muñoz, J.C. Chervin, N. Garro, D. Kim, Phys. Rev. B 74 (2006) 184301.
[22] M.K. Singh, S. Dussan, G.L. Sharma, R.S. Katiyar, J. Appl. Phys. 104 (2008) 113503.
[23] H. Gu, Y.Z. Jiang, Y.B. Xu, M. Yan, Appl. Phys. Lett. 98 (2011) 012502.
[24] K.S. Kim, Phys. Rev. B 11 (1975) 2177–2185.
[25] D.J. Aston, D.J. Payne, A.J.H. Green, R.G. Egdell, Phys. Rev. B 72 (2005) 195115.
[26] J.L. Cai, H. Gong, J. Appl. Phys. 98 (2005) 033707.
[27] D.W. Chu, Y.P. Zeng, D.L. Jiang, J. Phys. Chem. C 111 (2007) 5893–5897.
[28] A. Punnoose, H. Magnone, M.S. Seehra, J. Bonevich, Phys. Rev. B 64 (2001) 174420.
[29] J.M.D. Coey, M. Venkatesan, C.B. Fitzgerald, Nat. Mater. 4 (2005) 173.
[30] J. Tate, H.L. Ju, J.C. Moon, A. Zakutayev, A.P. Richard, J. Russell, D.H. McIntyre, Phys. Rev. B 80 (2009) 165206.
[31] C.Q. Sun, Nanoscale 2 (2010) 1930–1961.